SCIENTIFIC REPORTS

OPEN

SUBJECT AREAS:
APPLIED PHYSICS
ELECTROCATALYSIS
TWO-DIMENSIONAL MATERIALS
SENSORS

Received
21 September 2012

Accepted
15 January 2013

Published
13 February 2013

Correspondence and requests for materials should be addressed to M.Z.Z. (zhangmz@jlu.edu.cn)

Resonant tunneling modulation in quasi-2D Cu_2O/SnO_2 p-n horizontal-multi-layer heterostructure for room temperature H_2S sensor application

Guangliang Cui, Mingzhe Zhang & Guangtian Zou

State key laboratory of Superhard materials, Jilin University, Changchun 130012, P. R. China.

Heterostructure material that acts as resonant tunneling system is a major scientific challenge in applied physics. Herein, we report a resonant tunneling system, quasi-2D Cu_2O/SnO_2 p-n heterostructure multi-layer film, prepared by electrochemical deposition in a quasi-2D ultra-thin liquid layer. By applying a special half-sine deposition potential across the electrodes, Cu_2O and SnO_2 selectively and periodically deposited according to their reduction potentials. The as-prepared heterostructure film displays excellent sensitivity to H_2S at room temperature due to the resonant tunneling modulation. Furthermore, it is found that the laser illumination could enhance the gas response, and the mechanism with laser illumination is discussed. It is the first report on gas sensing application of resonant tunneling modulation. Hence, heterostructure material act as resonant tunneling system is believed to be an ideal candidate for further improvement of room temperature gas sensing.

Recent developments of nanoscience of effectively combining two or more chemically distinct components in one single nanostructure with multifunction or new properties induced by the heterointerfaces have led to revolutionary new applications of nanomaterials in various areas, such as catalysis, photovoltaic devices, sensors, and so on[1–3]. In particular, enormous efforts have been devoted to preparing heterostructured materials, including heterojunction nanocrystals, heterojunction nanowires and heterojunction arrays[4–6]. Heterojunction nanomaterials with multi-layer structure have multi-barrier structures which lead to periodic accumulation of carriers and control of their transport properties. They play an important role in modern device physics and have many practical applications[7,8]. One of such applications is to improve optical detection and gas sensing.

Conventional gas-sensing materials are used based on the change of carrier concentration caused by adsorption and desorption[9], which are functions of elevated operating temperature. Many of them do not have gas sensitivity at room temperature[10]. As a result, gas sensors often require a heating device to operate. Unfortunately, high temperature is harmful to the durability of sensors[11]. There have been considerable efforts to overcome the operating temperature limitation[12], such as using nanostructured materials with ultra-high surface-to-volume ratios, appropriate element doping, and surface decoration with noble metals[13–16]. Nevertheless, production of sensors operating at room temperature with high sensitivity, high selectivity, and low power consumption at nanowatt (nW) level remains a challenging task.

P-type Cu_2O[17] and N-type SnO_2[18] have been widely chosen as sensing materials in the last ten years. Their nanoscale materials, such as nanoparticle, nanowire and nanostructured film, have been investigated extensively for gas sensing applications[19–21]. With their small size, unique electrical properties, and high surface-to-volume ratios, they show excellent gas sensitivity at high temperatures. To improve the performance, we propose a Cu_2O/SnO_2 p-n heterostructure system. It is quasi-2D, having horizontal-multi-layer with strictly periodic structure in hundreds of microns composed of parallel one-dimensional Cu_2O and SnO_2 wire stripes. Different from previous reported heterojunction materials based on Cu_2O/CuO and SnO_2[22–24], our synthesized material can be considered as a resonant tunneling system with its application based on resonant tunneling modulation.

It is still hard to synthesize quasi-2D horizontal-multi-layer heterostructure with strictly periodic arrangement in hundreds of microns without using a template. Electrochemical deposition is an excellent method for synthesizing nanomaterials because the driving force of reaction is precisely controllable[25]. It is a good template-free approach to produce well-ordered nano/microstructure patterns[26,27], as we will show in the following discussion.

Results

We have made a quasi-2D Cu_2O/SnO_2 p-n horizontal-multi-layer heterostructure using selective deposition by applying a periodic potential in quasi-2D ultra-thin liquid layer. The selective deposition was achieved by applying a half-sine wave potential to the system and utilizing different deposition potentials of Cu_2O and SnO_2 (Figure 1b). The frequency of the half-sine wave was 0.5 Hz and the voltage varied from 0.3 to 0.9 V. The growth velocity was closely related to the concentration of electrolyte and applied potential[28]. Its cyclic growth pattern was caused by the variation of ion concentration near the growth front lagging behind the variation of electrode potential[29].

In the deposition process, hydroxide was first formed on the front of the deposit due to its lowest deposition potential. The reaction can be written as equation (1). Hydroxide was involved in the whole deposition process of Cu_2O and SnO_2 as the source of oxygen. Cu^{2+} and Sn^{2+} ions were driven by the electric field to the cathode, where they were reduced and deposited on the surface as adatoms. Cu_2O and SnO_2 nuclei started to nucleate, grow and assemble alternatively according to the periodic half-sine wave (Figure 1a), giving rise to crystallite agglomerates. They were selectively deposited at lower and upper parts of the half-sine wave, respectively. At the lower part of the half-sine wave, only Cu^{2+} can be deposited, as described in equation (2). During this deposition process, Cu^{2+} could migrate to the growth front in time as the deposition process was relatively slow. Therefore, the formed nanocrystals were large in size and easy to accumulate. As the deposition proceeds, the Cu^{2+} ions near the growth front were fully consumed, leaving Sn^{2+} ions in the growth interface. The accumulation of Sn^{2+} ions in the growth interface blocked the Cu^{2+} ions, eventually leading to a halt in the Cu_2O formation. Then, Sn^{2+} ions began to deposit when the voltage increased to large enough value, as described by equation (3). As the deposition process was relatively fast with high applied potential, Sn^{2+} could not migrate to the growth front rapidly enough to keep up with the rate of deposition, thus the formed nanocrystals were small in size with mild accumulation. Finally, the Sn^{2+} ions near the growth front were fully consumed, Cu^{2+} ions began to deposit in turn. This periodic deposition process led to the formation of ridgelike wires of Cu_2O and membrane stripes of SnO_2, alternating periodically.

$$NO_3^- + H_2O + 2e \rightarrow NO_2^- + 2OH^- \quad (1)$$

$$2Cu^{2+} + 2OH^- + 2e \rightarrow Cu_2O + H_2O \quad (2)$$

$$Sn^{2+} + 4OH^- \rightarrow SnO_2 + 2H_2O + 2e \quad (3)$$

Scanning electron micro-scope (SEM) images show a wavelike morphology of quasi-2D Cu_2O/SnO_2 p-n horizontal-multi-layer heterostructure (Figure 2a and Figure 2b). This multi-layer heterostructure shows a strictly periodic arrangement in hundreds of microns. Every cycle is composed of ridgelike wire and membrane stripe, which are symmetrical and well-ordered. The ridgelike wires are narrow, only about a quarter width of a cycle. Energy-dispersive X-ray spectroscopy (EDX) equipped on the transmission electron micro-scope (TEM) was used to measure both the composition profile of Cu and Sn in one cycle across the heterojunction (Figure 2c and Figure 2d). The line-profile analysis indicates that the Cu and Sn atoms are mainly distributed respectively at ridgelike wire and membrane stripe. The fluctuation of total signal intensity of Cu

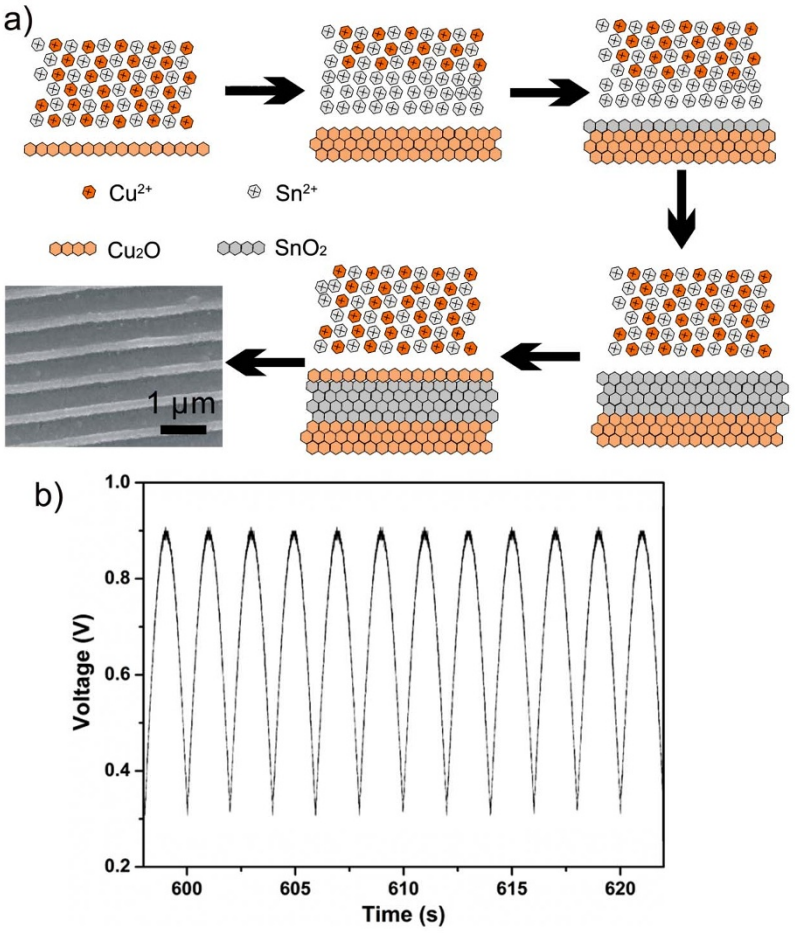

Figure 1 | Process of electrochemical deposition. (a) Schematic diagrams showing the electrochemical deposition process. (b) Half-sine waves applied across the electrodes in the electrochemical deposition process.

and Sn also reflects the cyclical variation in thickness of the heterostructure. The selective area electron diffraction (SAED) patterns of ridgelike wire and membrane stripe show polycrystalline rings corresponding to Cu_2O and SnO_2, respectively (Figure 2e and Figure 2g). No other components can be found. The result is consistent with the line-profile analysis. Figure 2f and Figure 2h are high-resolution transmission electron microscopy (HRTEM) images of SnO_2 and Cu_2O nanocrystals. The spacings of the fringes were measured to be 0.335 nm for SnO_2 and 0.246 nm for Cu_2O, corresponding to the (110) plane of SnO_2 and the (111) plane of Cu_2O. Moreover, these HRTEM images prove that the Cu_2O nanocrystal is significantly larger than SnO_2 nanocrystal.

In addition, X-ray photoelectron spectroscopy (XPS) was carried out to further confirm the presence of Cu_2O and SnO_2 (Figure 3a and Figure 3b). The distinct peak of 932.3 eV is assigned to Cu 2p core level, which can be used as a fingerprint to identify the presence of Cu^+. The peak with binding energy of 487.2 eV is consistent with Sn 3d core level spectrum, showing that stannum is in the form of Sn^{4+} state. No peaks of other chemical state of Cu and Sn are observed, indicating the high purity of this product. Both Cu_2O and SnO_2 are gas-sensing materials[19–21] with different behaviors to gases, and are conducive to distinction of different gases. The p-n heterojunction is the best choice because its barrier height is higher than that of other heterojunctions[30,31], which means a larger range of modulation. Both

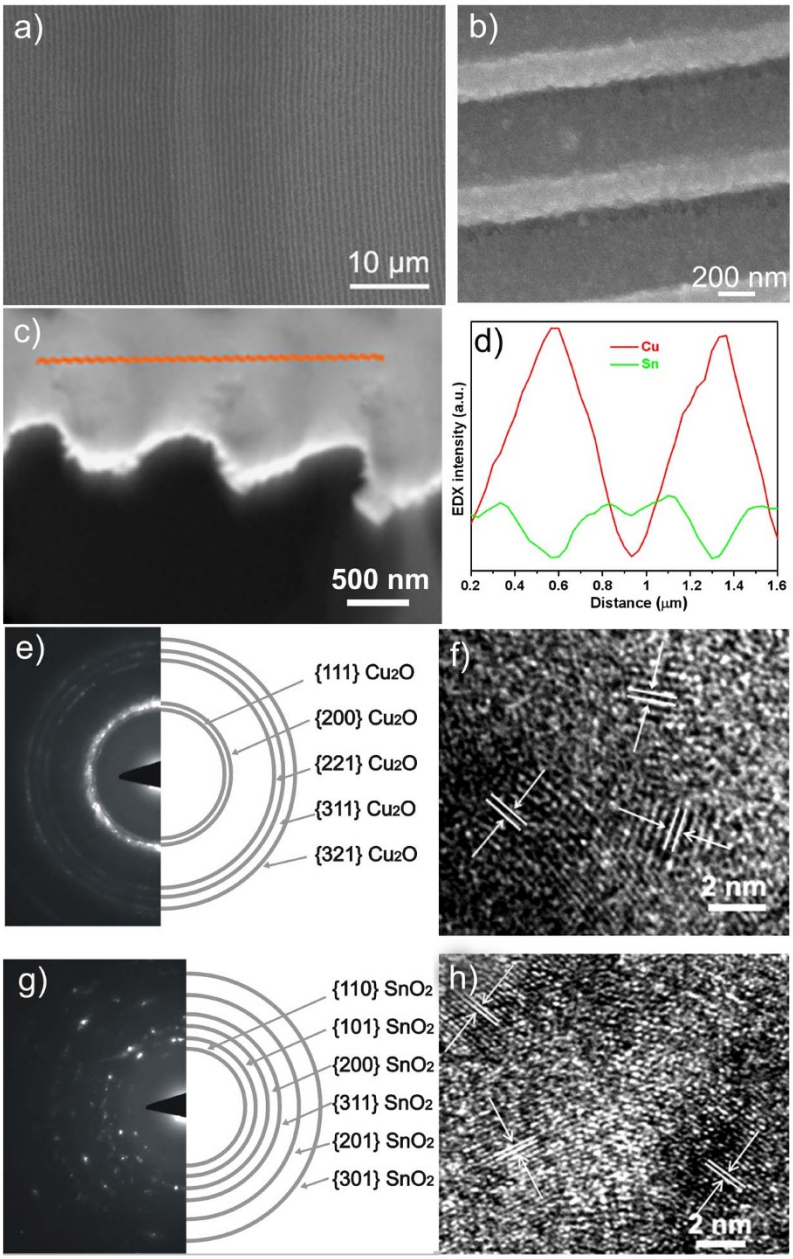

Figure 2 | Morphology and structure of quasi-2D Cu_2O/SnO_2 p-n horizontal-multi-layer heterostructure. (a) and (b): SEM images at low and high magnifications showing the wavelike morphology of quasi-2D Cu_2O/SnO_2 p-n horizontal-multi-layer heterostructure. (c) and (d): Line-profile analysis across the heterojunction as well as the distribution of Cu and Sn in one cycle. (e) and (g): SAED patterns of ridgelike wire and membrane stripes, which are corresponding to Cu_2O and SnO_2 respectively. (f) and (h): HRTEM images of SnO_2 and Cu_2O nanocrystals. The spacings of the fringes were measured to be 0.335 nm for SnO_2 and 0.246 nm for Cu_2O.

Cu_2O and SnO_2 are in the same plane, and both of them can interact with target gases and light illumination directly.

Discussion

The conductivity of quasi-2D Cu_2O/SnO_2 p-n horizontal-multi-layer heterostructure was characterized by electrical measurements at various temperatures. The circuit schematic diagram and *I-V* curves are shown in Figure 3c and 3d, respectively. The investigation show that the conductivity increased first and then decreased as the temperature rising from 10 K to 260 K, with a maximum at 110 K. The enhanced conductivity was due to increased carrier concentration with increasing temperature. However, p-n heterojunction barrier height increased much more rapidly with increasing temperature[32], and ultimately controls the conductivity of p-n multi-layer heterostructure, leading to the decrease of conductivity. Hence, the conductivity of Cu_2O/SnO_2 p-n horizontal-multi-layer heterostructure is mainly controlled by its barrier height near room temperature.

The special structure of the quasi-2D Cu_2O/SnO_2 p-n horizontal-multi-layer heterostructure determines its excellent gas sensing performance, especially for H_2S at room temperature. The *I–V* curves of a typical sensor in air and 50 ppm H_2S in air exhibit obvious non-linear characteristics at room temperature, indicating the presence of multi-barrier (Figure 4a). Notably, the current in air is in the range of 10^{-8} A, which is low and enhances the sensitivity of the sensor[33]. The low conductivity is mainly attributed to the superimposed effect of the multi-barrier. The conductivity increased obviously when the sensor was exposed to 50 ppm H_2S. Our multi-layer heterostructure shows a reversible resistance change (ΔR) relative to the original value (R) over many cycles. As shown in Figure 4b, the response of sensor to 50 ppm H_2S can reach about 45% at room temperature. While the sensor responses to 50 ppm liquefied petroleum gas (LPG), NH_3, NO, H_2 and toluene in air are much weaker. Their *I–V* curves at room temperature are shown in Supplementary Figure S2. The superior sensitivity ($\Delta R/R$) and selectivity of the sensor to H_2S are evident from Figure 4b. Figure 4c shows dynamic responses of the sensor to 50 ppm H_2S in air at room temperature. Upon exposure to the H_2S, the sensitivity increased fast, and then reached saturation rapidly. Similarly, the sensitivity sharply reduced as soon as the gas was turned off. It can be observed in the figure 4d that the sensor has a wide detection range for H_2S from 0.5 to 100 ppm at room temperature. The response increases linearly with increasing H_2S concentration between 0.5 and 100 ppm. Above 100 ppm, the response has no significant change, indicating that the response becomes saturated. Notably, the sensor has reasonable response to 0.5 ppm H_2S in air, so the detection limit of the sensor can reach as little as sub-ppm to H_2S at room temperature. The excellent sensitivity to sub-ppm concentration H_2S is due to the advanced tunneling modulation mechanism, which makes our sensor highly successful comparing with other sensors.

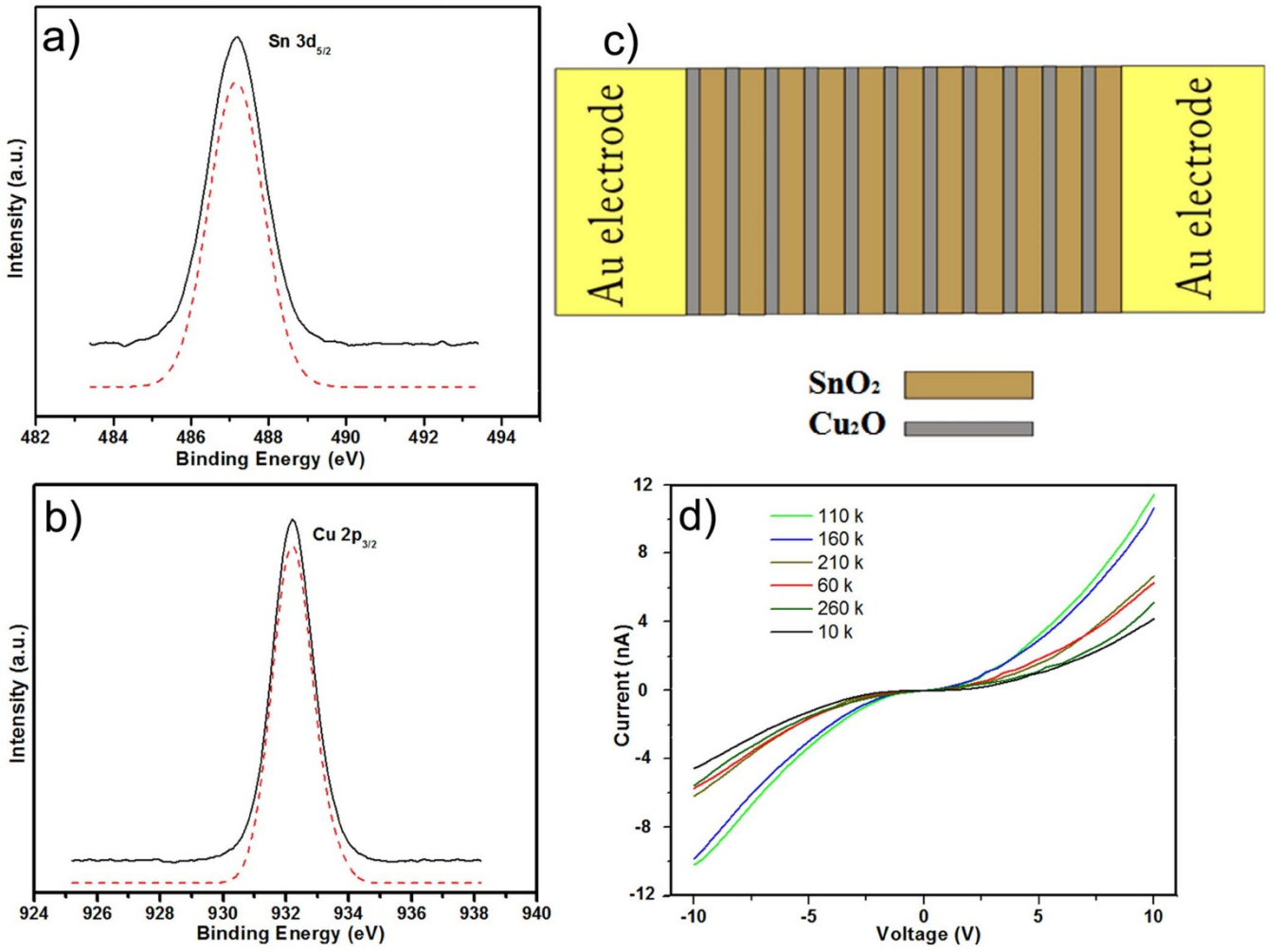

Figure 3 | Sn 3d and Cu 2p XPS spectra and temperature-dependent conductivity of quasi-2D Cu_2O/SnO_2 p-n horizontal-multi-layer heterostructure. (a) and (b): Curve-fitting results of the Sn 3d and Cu 2p XPS spectra. (c) The schematic diagram of typical sensor. (d) *I–V* curves of the Cu_2O/SnO_2 p-n horizontal-multi-layer heterostructure at various temperatures.

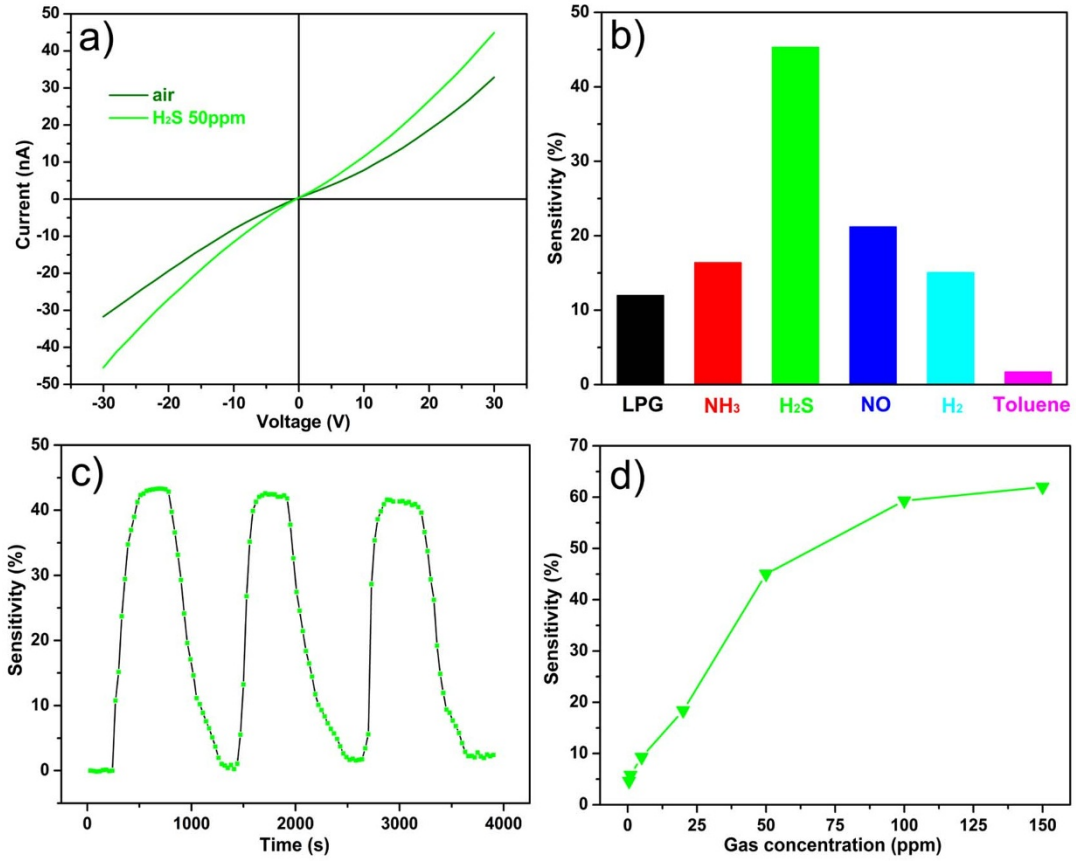

Figure 4 | Performance of typical sensor based on the quasi-2D Cu_2O/SnO_2 p-n horizontal-multi-layer heterostructure at room temperature. (a) *I–V* curves of the sensor to 50 ppm H_2S in air. (b) The sensitivities of the sensor to 50 ppm LPG, NH_3, H_2S, NO, H_2 and toluene in air. (c) Dynamic responses of the sensor to 50 ppm H_2S in air. (d) The H_2S concentration dependence of the sensor.

The sensitivity of gas sensing materials depends on the extent of adsorption and desorption, while the response and recovery time depend on the speed of adsorption and desorption processes. Although the room temperature sensitivity of the sensor is greatly improved, the response and recovery behaviors are not quite optimized. Considering the above situation, we introduce laser illumination. As shown in Figure 5a, under 50 ppm H_2S condition, the conductivity of the sensor with laser illumination exhibits an obvious increase. Figure 5b shows the response of sensor to 50 ppm H_2S in air at room temperature is improved by almost 20% (from 45% to 65.1%) with laser illumination, while no obvious improvement are observed to other gases (Supplementary Table S1 and Figure S1). The *I–V* curves of the sensor to 50 ppm LPG, NH_3, NO, H_2 and toluene in air with laser illumination at room temperature were shown in Supplementary Figure S3. Moreover, the response and recovery time are significantly reduced from 180 to 160 s and from 500 to 240 s compared with that of no laser illumination, as shown in Figure 5c. This suggests that the speed of adsorption and desorption processes are accelerated under laser illumination. It can be found in the figure 5d that the sensor has a relative narrow detection range for H_2S from 0.5 to 50 ppm with laser illumination at room temperature. The response increases linearly with increasing H_2S concentration below 50 ppm. Above 50 ppm, the response has no significant change, indicating that the response becomes saturated. The response ceiling of the sensor is brought forward from 100 to 50 ppm with laser illumination (Supplementary Figure S4). This demonstrates that the adsorption is enhanced by the laser illumination. In summary, the sensor has excellent performance for sensing H_2S at room temperature, and it could be further improved with laser illumination.

The quasi-2D Cu_2O/SnO_2 p-n horizontal-multi-layer heterostructure is a multi-barrier system, where carriers transport by resonant tunneling. When it is exposed to H_2S, part of the absorbed oxygen atoms on the surface of Cu_2O and SnO_2 are removed, leaving oxygen-bound electrons in the surface. As a result, the free electron concentration of SnO_2 increased, while the hole concentration of Cu_2O decreased. Because of the reduction of hole concentration, the carrier diffusion between SnO_2 and Cu_2O reduced, leading to narrower depletion layer of the p-n heterojunction. Finally, the heterojunction barrier decreases for the changed Fermi level. Therefore, electrons have a relatively large probability of crossing the multi-barrier by resonant tunneling. Because the adsorption and desorption are functions of operating temperature[9], the change of carrier concentration is limited at room temperature. However, the conductivity of Cu_2O/SnO_2 p-n horizontal-multi-layer heterostructure depends on heterojunction barrier, which is sensitive to the carrier concentration[34]. Hence, the resonant tunneling modulation requires a low level change of carrier concentration. The resonant tunneling modulation process is very rapid and easy to restore, even at room temperature. Hence, room temperature sensitivity to H_2S can be obtained by the application of Cu_2O/SnO_2 p-n horizontal-multi-layer heterostructure. Further, if the application of resonant tunneling modulation in gas sensing can be implemented, it will make significant advances in room temperature gas sensing. The nano size of Cu_2O and SnO_2 crystals and wavelike morphology with large surface areas also contribute to the superior room temperature sensitivity.

When the laser illumination is applied, it is necessary to determine whether the sensitivity changes are caused by thermal or nonthermal mechanisms. If it is from the heating of laser illumination, its rate should be a function of energy deposited on the sensor. As shown in

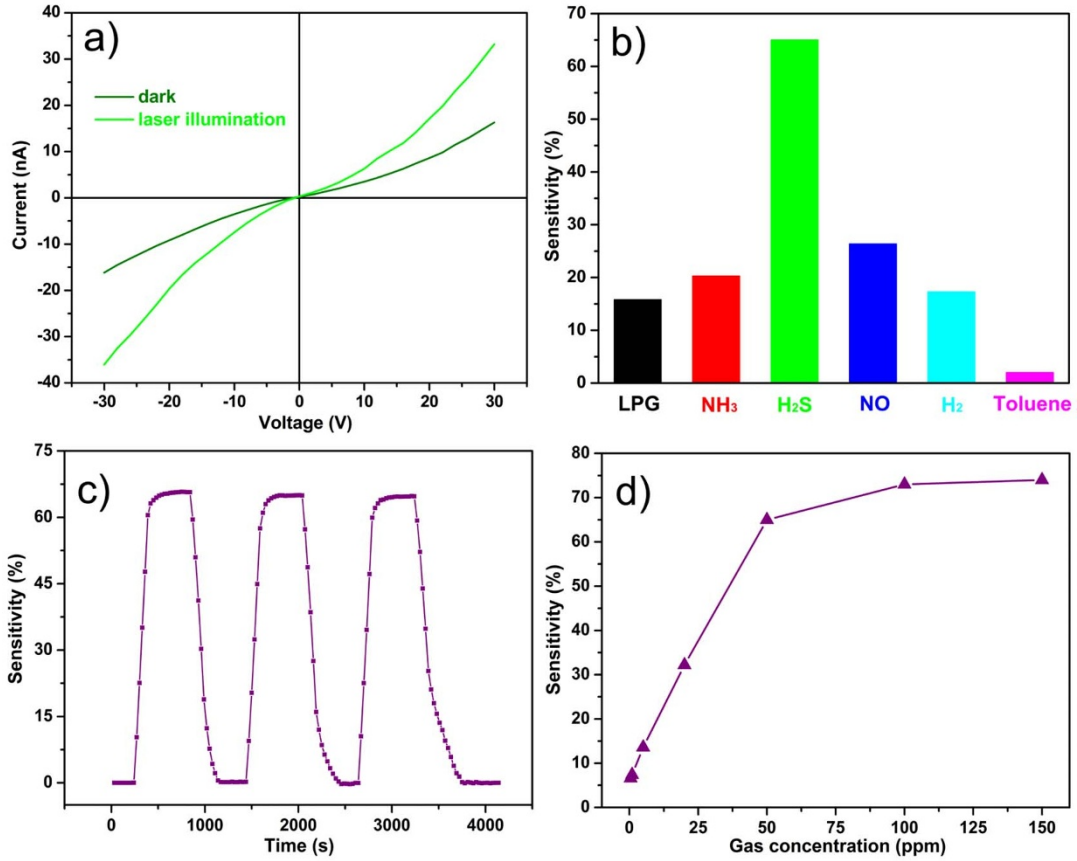

Figure 5 | Performance of typical sensor based on the quasi-2D Cu_2O/SnO_2 p-n horizontal-multi-layer heterostructure with laser illumination (405 nm, 20 mW•cm^{-2}) at room temperature. (a) *I–V* curves of the sensor to 50 ppm H_2S in air with laser illumination. (b) The sensitivities of the sensor to 50 ppm LPG, NH_3, H_2S, NO, H_2 and toluene in air with laser illumination. (c) Dynamic responses of the sensor to 50 ppm H_2S in air with laser illumination. (d) The H_2S concentration dependence of the sensor with laser illumination.

Figure 6a, the response of sensor to 50 ppm H_2S in air is 45% without laser illumination, and 60.1% under laser illumination with the power of 5 mW•cm^{-2}. However, the response is not significantly increased with the increase of the power. Therefore, the improved gas sensitivity with laser illumination is not caused by the heating effect of laser. Only laser illumination cannot lead to such a substantial increase of conductivity. Conductivity increased slightly only under laser illumination at room temperature (Figure 6b). We believe that the increased sensitivity is due to a synergistic effect of laser illumination and H_2S.

The laser illumination excites the electron-hole pairs on the surface of Cu_2O and SnO_2, which increases the conductivity of materials, and also modifies the electric field due to charge accumulation near the heterojunction barriers[35]. The conductivity of Cu_2O/SnO_2 p-n horizontal-multi-layer heterostructure is improved with laser illumination, which makes the change of conductivity caused by H_2S more obvious. More important, laser illumination reduces the energy barrier of desorption[36], causing further reduction of heterojunction barrier. Accordingly, resonant tunneling modulation is greatly improved with laser illumination for the enhanced interaction between material and gas. At the same time, the improvement of desorption speed leads to the acceleration of response behavior. All these contribute to the increase of sensitivity. On the other hand, the sensitivity of sensor due to laser illumination doesn't seem to apply to other gases, so the selectivity is retained and improved with laser illumination.

In summary, we fabricate a quasi-2D Cu_2O/SnO_2 p-n horizontal-multi-layer heterostructure with strictly periodic arrangement in hundreds of microns which can be considered as a resonant tunneling system. Our work makes a breakthrough in gas-sensing application of resonant tunneling modulation. The resonant tunneling modulation in this system can be achieved at room temperature by H_2S irritation. The detection limit of sensor based on this heterostructure system can reach as little as sub-ppm to H_2S at room temperature. Compared with the existing room temperature H_2S sensors[37–40], our sensors are based on the advanced tunneling modulation mechanism, and have higher sensitivity and selectivity to low concentration (sub-ppm) H_2S at room temperature. Moreover, the response and recovery time are much shorter for the agility of resonant tunneling modulation at room temperature. Notably, Laser illumination also improves the sensor performance. Therefore, this kind of p-n multi-layer heterostructure provides a new direction of designing materials for room temperature gas sensing.

Methods

Preparation. The Quasi-2D Cu_2O/SnO_2 p-n horizontal-multi-layer heterostructure was synthesized by an electronchemical deposition system in a quasi-2D ultra-thin electrolyte liquid layer. This system consisted of a growth chamber, a low-temperature cycle water bath (Polystat, Cole-parmer, USA), a dc power supply (DF1731SB5A, Zhongce, China), an arbitrary function generator (AFG310, Tektronix, USA), and a CCD camera (A311f, Leica, Germany). The electrolyte was prepared using analytical reagent $Cu(NO_3)_2$, $SnCl_2$ and Millipore water. The ion concentrations of Cu^{2+} and Sn^{2+} in electrolyte were 0.08 M and 0.02 M respectively. The pH value was adjusted to 2.4 by nitricacid. The Si substrate was first oxidized to form a layer of SiO_2 on the surface, and the SiO_2 layer was used to protect the electron transport from the substrate. Two parallel Cu foil electrodes (30 μm-thick, 99.9%) were put on the Si substrate, which was placed on the Peltier element in the growth chamber. Then the prepared solution was added dropwise. After that, a cover glass was carefully put on the two electrodes, and ensures the space between the coverglass and the SiO_2/Si substrate was filled with electrolyte. The Peltier element and low-temperature cycle water bath were used to control the temperature and solidify the

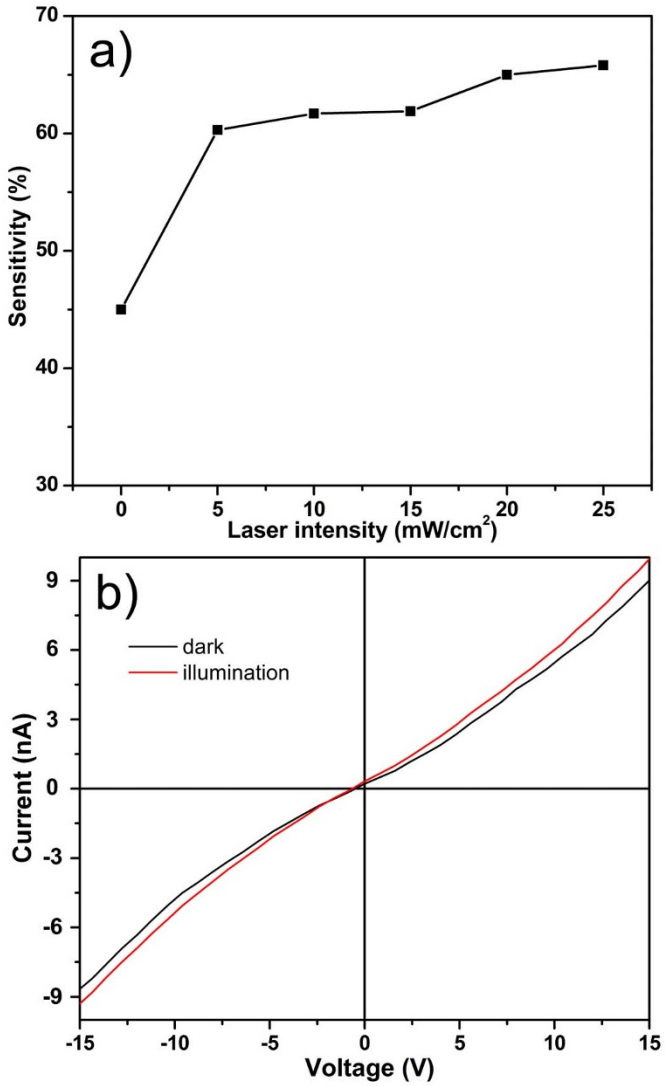

Figure 6 | Expression of Laser illumination effect to sensor. (a) The sensitivities of sensor to 50 ppm H_2S in air with various laser (405 nm) intensities at room temperature. (b) *I–V* curves of sensor with and without laser illumination (405 nm, 20 mW·cm^{-2}).

electrolyte. An ultra-thin ice layer could be formed between the silicon substrate and the cover glass by adjusting the temperature of the Peltier element and low-temperature cycle water bath accurately. The solute in the electrolyte was partially expelled from the solid in the solidification process due to the partitioning effect. Eventually two ultra-thin liquid layers of concentrated electrolyte were formed between the ice layer and the lower silicon substrate as well as the ice layer and the higher cover glass separately. The thickness of the ultra-thin electrolyte layers are about 300 nm, and the electrodeposition process was carried at −4.5°C by applying a half-sine wave potential (0.3–0.9 V) with a frequency of 0.5 Hz across the ultra-thin liquid layers. The growth time is about 1 h, during which the real-time growth process can be observed by the optical microscope (Leica Dmlm). When the growth process finished, the coverglass and silicon wafer were taken out, and cleaned by the Millipore water. Finally, Cu_2O/SnO_2 p-n heterostructure left on the surface of coverglass and Si substrate. The as-prepared quasi-2D Cu_2O/SnO_2 horizontal-multi-layer heterostructure was examined by field-emission SEM (JSM-6700F, JEOL, Japan), TEM (Tecnai G2, FEI, USA), and XPS (ESCALAB MKII, VG, UK) for morphology, composition, crystallography, and structure characterization, respectively.

Gas sensitivity test. The samples on the cover glass were chosen as the test object. First, the sample was covered by a linear mask with a width of 100 μm and parallel to the heterointerface. Two copper wires were fixed on both sides of the mask separately. Then the Au film was deposited on the glass by vacuum ion sputtering for 300 s. After that, the mask was taken away, and the heterostructure system was connected into the circuit. The target gases with desired concentrations were prepared by static volumetric method. The gas response measurements were carried out in a vacuum test system, including a test chamber, optical platform, laser source and an air pump. The sensor was kept in the test chamber equipped with appropriate optical window, inlets and outlets for laser and target gases flow, and the air and target gases were alternately introduced into the test chamber. During the measurement, the electrical signals were recorded every 30 seconds by a Keithley 2400 sourcemeter (2400, Keithley, USA) and a Digital Phosphor Oscilloscope (TDS5034B, Tektronix, USA) under laser (405 nm) illumination with a low power density of 20 mW·cm^{-2}.

1. Tada, H., Mitsui, T., Kiyonaga, T., Akita, T. & Tanaka, K. All-Solid-State Z-Scheme in CdS-Au-TiO_2 Three-Component Nanojunction System. *Nat. Mater.* **5**, 782–786 (2006).
2. Khalavka, Y. & Sönnichsen, C. Growth of Gold Tips onto Hyperbranched CdTe Nanostructures. *Adv Mater* **20**, 588–591 (2008).
3. Amirav, L. & Alivisatos, A. P. Photocatalytic hydrogen production with tunable nanorod heterostructures. *J. Phys. Chem. Lett.* **1**, 1051–1054 (2010).
4. Beveridge, J. S., Buck, M. R., Bondi, J. F., Misra, R., Schiffer, P., Schaak, R. E. & Williams, M. E. Purification and Magnetic Interrogation of Hybrid Au-Fe_3O_4 and FePt-Fe_3O_4 Nanoparticles. *Angewandte Chemie* **123**, 10049–10053 (2011).
5. Perea, D. E., Li, N., Dickerson, R. M., Misra, A. & Picraux, S. T. Controlling Heterojunction Abruptness in VLS-Grown Semiconductor Nanowires via in situ Catalyst Alloying. *Nano Lett.* **11**, 3117–3122 (2011).
6. Park, W. I. & Yi, G. C. Electroluminescence in n-ZnO Nanorod Arrays Vertically Grown on p-GaN. *Adv Mater* **16**, 87–90 (2004).
7. Jeong, M. C., Oh, B. Y., Ham, M. H. & Myoung, J. M. Electroluminescence from ZnO nanowires in n-ZnO film/ZnO nanowire array/p-GaN film heterojunction light-emitting diodes. *Appl Phys Lett* **88**, 202105 (2006).
8. Huang, H., Gong, H., Chow, C. L., Guo, J., White, T. J., Tse, M. S. & Tan, O. K. Low-Temperature Growth of SnO_2 Nanorod Arrays and Tunable n–p–n Sensing Response of a ZnO/SnO_2 Heterojunction for Exclusive Hydrogen Sensors. *Adv Funct Mater* **21**, 2680–2686 (2011).
9. Salunkhe, R. R., Shinde, V. R. & Lokhande, C. D. Liquefied petroleum gas (LPG) sensing properties of nanocrystalline CdO thin films prepared by chemical route: Effect of molarities of precursor solution. *Sensor Actuat. B-Chem.* **133**, 296–301 (2008).
10. Soulantica, K., Erades, L., Sauvan, M., Senocq, F., Maisonnat, A. & Chaudret, B. Synthesis of indium and indium oxide nanoparticles from indium cyclopentadienyl precursor and their application for gas sensing. *Adv Funct Mater* **13**, 553–557 (2003).
11. Davis, S. R., Chadwick, A. V. & Wright, J. D. The effects of crystallite growth and dopant migration on the carbon monoxide sensing characteristics of nanocrystalline tin oxide based sensor materials. *J. Mater. Chem.* **8**, 2065–2071 (1998).
12. Lu, G. H., Ocola, L. E. & Chen, J. H. Room-Temperature Gas Sensing Based on Electron Transfer between Discrete Tin Oxide Nanocrystals and Multiwalled Carbon Nanotubes. *Adv Mater* **21**, 2487–2491 (2009).
13. Liu, Y. G., Feng, P., Xue, X. Y., Shi, S. L., Fu, X. Q., Wang, C., Wang, Y. & Wang, G. T. H. Room-temperature oxygen sensitivity of ZnS nanobelts. *Appl Phys Lett* **90**, 042109 (2007).
14. Dimova-Malinovska, D., Nichev, H., Georgieva, V., Angelov, O., Pivin, J. C. & Mikli, V. Sensitivity of ZnO films doped with Er, Ta and Co to NH_3 at room temperature. *Phys Status Solidi A* **205**, 1993–1997 (2008).
15. Ren, S. T., Fan, G. H., Qu, S. L. & Wang, Q. Enhanced H_2 sensitivity at room temperature of ZnO nanowires functionalized by Pd nanoparticles. *J Appl Phys* **110**, 084312 (2011).
16. Cui, G. L., Li, Z. M., Gao, L. & Zhang, M. Z. CdO nanosheet film with a (200)-preferred orientation with sensitivity to liquefied petroleum gas (LPG) at low-temperatures. *Phys. Chem. Chem. Phys.* **14**, 16321–16325 (2012).
17. Paracchino, A., Laporte, V., Sivula, K., Gratzel, M. & Thimsen, E. Highly active oxide photocathode for photoelectrochemical water reduction. *Nat Mater* **10**, 456–461 (2011).
18. Lou, X. W., Wang, Y., Yuan, C. L., Lee, J. Y. & Archer, L. A. Template-free synthesis of SnO_2 hollow nanostructures with high lithium storage capacity. *Adv Mater* **18**, 2325–2329 (2006).
19. Scott, R. W. J., Yang, S. M., Chabanis, G., Coombus, N., Williams, D. E. & Ozin, G. A. Tin Dioxide Opals and Inverted Opals: Near-Ideal Microstructures for Gas Sensors. *AdV. Mater.* **13**, 1468–1472 (2001).
20. Lee, W. S., Lee, S. C., Lee, S. J., Lee, D. D., Huh, J. S., Jun, H. K. & Kim, J. C. The sensing behavior of SnO_2-based thick-film gas sensors at a low concentration of chemical agent stimulants. *Sens. Actuators, B* **108**, 148–153 (2005).
21. Kuang, Q., Lao, C. S., Wang, Z. L., Xie, Z. X. & Zheng, L. S. High-sensitivity humidity sensor based on a single SnO_2 nanowire. *J. Am. Chem. Soc.* **129**, 6070–6071 (2007).
22. Chowdhuri, A., Gupta, V., Sreenivas, K., Kumar, R., Mozumdar, S. & Patanjali, P. K. Response speed of SnO_2-based H_2S gas sensors with CuO nanoparticles. *Appl Phys Lett* **84**, 1180–1182 (2004).
23. Khanna, A., Kumar, R. & Bhatti, S. S. CuO-doped SnO_2 thin films as hydrogen sulfide gas sensor. *Appl Phys Lett* **82**, 4388–4390 (2003).
24. Xue, X. Y., Xing, L. L., Chen, Y. J., Shi, S. L., Wang, Y. G. & Wang, T. H. Synthesis and H_2S sensing properties of CuO-SnO_2 core/shell PN-junction nanorods. *J Phys Chem C* **112**, 12157–12160 (2008).

25. Switzer, J. A., Hung, C. J., Breyfogle, B. E., Shumsky, M. G., Vanleeuwen, R. & Golden, T. D. Electrodeposited defect chemistry superlattices. *Science*, **264**, 1573–1576 (1994).
26. Zhang, M. Z., Zuo, G. L., Zong, Z. C., Cheng, H. Y., He, Z., Yang, C. M. & Zou, G. T. Self-assembly of copper micro/nanoscate parallel wires by electrode position on a silicon substrate. *Small* **2**, 727–731 (2006).
27. Zong, Z. C., Liu, J. Y., Hu, T. T., Li, D. D., Tian, H. F., Liu, C., Zhang, M. Z. & Zou, G. T. PbTe/Pb quasi-one-dimensional nanostructure material: controllable array synthesis and side branch formation by electrochemical deposition. *Nanotechnology* **21**, 185302 (2010).
28. Liu, C., Yao, B. B., Wang, S. M., Tian, H. F. & Zhang, M. Z. Fabrication of the Pattern of Copper Nanowires with Adjustable Density on Oxidized Si Substrate. *J Phys Chem C* **113**, 21303–21307 (2009).
29. Zong, Z. C., Yu, H., Niu, L. P., Zhang, M. Z., Wang, C., Li, W., Men, Y. F., Yao, B. B. & Zou, G. T. Potential-induced copper periodic micro-/nanostructures by electrodeposition on silicon substrate. *Nanotechnology* **19**, 315302 (2008).
30. Duan, X. F., Huang, Y., Cui, Y., Wang, J. F. & Lieber, C. M. Indium phosphide nanowires as building blocks for nanoscale electronic and optoelectronic devices. *Nature* **409**, 66–69 (2001).
31. Duan, X. F., Huang, Y., Agarwal, R. & Lieber, C. M. Single-nanowire electrically driven lasers. *Nature* **421**, 241–245 (2003).
32. Majumdar, S. & Banerji, P. Temperature dependent electrical transport in p-ZnO/n-Si heterojunction formed by pulsed laser deposition. *J. Appl. Phys.* **105**, 043704 (2009).
33. Tsang, S. W., Denhoff, M. W., Tao, Y. & Lu, Z. H. Charge-carrier induced barrier-height reduction at organic heterojunction. *Phys. Rev. B* **78**, 081301 (2008).
34. Wang, R. C., Lin, H. Y., Wang, C. H. & Liu, C. P. Fabrication of a Large-Area Al-Doped ZnO Nanowire Array Photosensor with Enhanced Photoresponse by Straining. *Adv. Funct. Mater.* **22**, 3875–3881 (2012).
35. Park, P. W., Chu, H. Y., Han, S. G., Choi, Y. W., Kim, G. & Lee, E. H. Optical switching mechanism based on charge accumulation effects in resonant tunneling diodes. *Appl. Phys. Lett.* **67**, 1241 (1995).
36. Li, J., Lu, Y. J., Ye, Q., Cinke, M., Han, J. & Meyyappan, M. Carbon nanotube sensors for gas and organic vapor detection. *Nano Lett* **3**, 929–933 (2003).
37. Solis, J. L., Saukko, S., Kish, L. B., Granqvist, C. G. & Lantto, V. Nanocrystalline tungsten oxide thick-films with high sensitivity to H_2S at room temperature. *Sens. Actuators, B* **77**, 316–321 (2001).
38. Kong, X. H. & Li, Y. D. High sensitivity of CuO modified SnO_2 nanoribbons to H_2S at room temperature. *Sens. Actuators B* **105**, 449–453 (2005).
39. Tong, M. S., Dai, G. R., Wu, Y. D. & Gao, D. S. High sensitivity and switching-like response behavior of SnO_2–Ag–SnO_2 element to H_2S at room temperature. *J. Mater. Sci. Mater. Electron.* **11**, 61–665 (2000).
40. Zhang, N., Yu, K., Li, Q., Zhu, Z. Q. & Wan, Q. Room-temperature high-sensitivity H_2S gas sensor based on dendritic ZnO nanostructures with macroscale in appearance. *J. Appl. Phys.* **103**, 104305 (2008).

Acknowledgments

This work was funded by the National Science Foundation of China, Nos. 90923032, 11174103 and 20873052.

Author contributions

M.Z.Z. conceived and designed the experiments. G.L.C. performed the experiments. M.Z.Z., G.T.Z. and G.L.C. interpreted the results. All authors co-wrote the manuscript.

Additional information

Supplementary information accompanies this paper at http://www.nature.com/scientificreports

Competing financial interests: The authors declare no competing financial interests.

How to cite this article: Cui, G.L., Zhang, M.Z. & Zou, G.T. Resonant tunneling modulation in quasi-2D Cu_2O/SnO_2 p-n horizontal-multi-layer heterostructure for room temperature H_2S sensor application. *Sci. Rep.* **3**, 1250; DOI:10.1038/srep01250 (2013).